Water-Stable, Magnetic Silica–Cobalt/Cobalt Oxide–Silica Multishell Submicrometer Spheres

ARTICLE *in* ADVANCED FUNCTIONAL MATERIALS · JUNE 2005

Impact Factor: 11.81 · DOI: 10.1002/adfm.200400469

3 AUTHORS, INCLUDING:

Marina Spasova
University of Duisburg-Essen
84 PUBLICATIONS **2,406** CITATIONS
SEE PROFILE

Michael Farle
University of Duisburg-Essen
260 PUBLICATIONS **5,967** CITATIONS
SEE PROFILE

DOI: 10.1002/adfm.200500565

Composite Silica Spheres with Magnetic and Luminescent Functionalities**

By *Verónica Salgueiriño-Maceira*,* *Miguel A. Correa-Duarte*, *Marina Spasova*, *Luis M. Liz-Marzán*, and *Michael Farle*

A new class of highly fluorescent, photostable, and magnetic core/shell nanoparticles in the submicrometer size range has been synthesized from a modified Stöber method combined with the layer-by-layer (LbL) assembly technique. Luminescent magnetic nanoparticles are prepared via two main steps. The first step involves controlled addition of tetraethoxysilane to a dispersion of Fe_3O_4/γ-Fe_2O_3 nanoparticles, which are thereby homogeneously incorporated as cores into monodisperse silica spheres. The second step involves the LbL assembly of polyelectrolytes and luminescent CdTe quantum dots onto the surfaces of the silica-coated magnetite/maghemite particles, which are finally covered with an outer shell of silica. These spherical particles have a typical diameter of 220 ± 10 nm and a saturation magnetization of 1.34 emu g^{-1} at room temperature, and exhibit strong excitonic photoluminescence. Nanoparticles with such a core/shell architecture have the added benefit of providing a robust platform (the outer silica shell) for incorporating diverse functionalities into a single nanoparticle.

1. Introduction

Colloidal II–VI semiconductor nanocrystals, known as quantum dots (QDs), have gained increasing attention in technological applications and fundamental studies because of their unique optical properties.[1] Because of their strong bandgap luminescence, which is tunable by varying the particle size (as a result of the quantum-confinement effect), colloidally synthesized semiconductor nanoparticles are currently of great interest as light-emitting materials for biolabeling applications.[2] The fundamental drawback of most syntheses is that the particles produced are luminescent and photostable only in nonpolar media, which means that biological applications are hindered. Different methods to transfer these luminescent materials into water have been developed, but often the photostability of the QDs becomes drastically reduced in oxygenated aqueous solution. If they are to be solubilized in aqueous buffers, their hydrophobic surface ligands must be replaced by amphiphilic ones and different QD solubilization strategies have been devised over the past few years, including: a) ligand exchange with simple thiol-containing molecules[2b,3] or more sophisticated ones;[4] b) encapsulation by a layer of amphiphilic diblock or triblock copolymers[5] or in silica shells,[2a,d] polymer shells,[6] or amphiphilic polysaccharides;[7] and c) combining layers of different molecules conferring the required colloidal stability to the QDs.[2c] Alternative methods have been reported for the synthesis of water-based QDs[8] and Rogach and coworkers[9] were able to synthesize water-based thiol-capped CdTe nanocrystals with very stable luminescence covering almost the entire visible spectral range (450–750 nm), depending on particle size. Magnetic nanoparticles have been widely used in different fields, including advanced technological areas and biology. This field of biomagnetics is rapidly growing and consists of a broad range of current applications, including labeling and sorting of cells,[10] cell separation,[11] separation of biochemical products,[12] biosensing,[13] studies of cellular function,[14] as well as a variety of potential medical and therapeutic applications.[15] Iron oxide nanoparticles consisting of maghemite (γ-Fe_2O_3) or magnetite (Fe_3O_4) have been of great interest not only for the study of fundamental magnetic properties, but also for biomedical applications. Nevertheless, the reactivity of iron oxide nanoparticles has been shown to greatly increase as their dimensions are reduced, and particles with relatively small sizes may undergo rapid biodegradation when they are directly exposed to biological environments. Therefore, a suitable coating is essential to overcome such limitations, and encapsulation with silica endows the nanomagnets with several beneficial properties for their use in biomedical applications. These properties include compatibility in biological systems,[16] functionality, high colloidal stability under different conditions, the ability to modulate the magnetic properties with heating, and hydrophilicity.[17] A further benefit of using inorganic coat-

[*] Dr. V. Salgueiriño-Maceira, Dr. M. Spasova, Prof. M. Farle
Fachbereich Physik, Universtität Duisburg-Essen
47048 Duisburg (Germany)
E-mail: veronica@ttphysik.uni-duisburg.de
Dr. V. Salgueiriño-Maceira
Instituto de Investigacións Tecnolóxicas
Universidade de Santiago de Compostela
15782, Santiago de Compostela (Spain)
Dr. M. A. Correa-Duarte, Prof. L. M. Liz-Marzán
Departamento de Química Física, Universidade de Vigo
36310, Vigo (Spain)

[**] V. S.-M. and M. A. C.-D. acknowledge financial support from the *Isidro Parga Pondal* Programme (Xunta de Galicia, Spain). L. M. L.-M. and M. F. gratefully acknowledge the European Community's Marie-Curie Research Training Network SyntOrbMag (contract No. MRTN-CT-2004-005567).

ings in general, and silica in particular, is the resulting delayed conversion of γ-Fe_2O_3 to the thermodynamically stable form, α-Fe_2O_3.[18] Silica coatings have been applied to a multitude of systems, including gold and silver nanoparticles,[19] rods,[20] carbon nanotubes,[21] and QDs.[2a,22] Moreover, surface silanol groups can easily react with alcohols and silane coupling agents, not only to produce stable dispersions in non-aqueous solvents, but also to provide ideal anchorage for the covalent binding of specific ligands. This becomes very important, since the main applications of magnetic carriers are derived from the fact that specific ligands (streptadivin, antibodies, etc.) can be covalently bound to the magnetic carrier enabling binding to various target substances/organs such as cells, proteins, and nucleic acids, as well as perform antibody–antigen recognition.

In this paper, the interest arises from the possibility of combining optical and magnetic properties by entrapping magnetic and semiconductor nanoparticles in the same silica spheres, using a reproducible and feasible method that provides highly stable and luminescent markers with narrow emission bands located at desired wavelengths, and that are easily manipulated by an external magnetic field.

2. Results and Discussion

Magnetic and luminescent nanocomposite particles were prepared by a successive combination of the base-catalyzed hydrolysis of tetraethyl orthosilicate (TEOS) onto iron oxide nanoparticles (10 nm average diameter) and layer-by-layer (LbL) assembly, which drives CdTe QDs (3–5 nm average diameter) onto the surfaces of magnetic particles previously coated with silica, as outlined in Scheme 1.

Magnetite nanoparticles (which were partially oxidized to maghemite according to an X-ray diffraction study, not shown) were trapped within silica spheres using a sol–gel method based on the hydrolysis of TEOS, which relies on the well-known Stöber method,[23] forming uniform core/shell units (Scheme 1A). Because the iron oxide surface has a strong affinity to silica, no primer was required to promote the deposition and adhesion of silica.[24] Figure 1 shows transmission electron microscopy (TEM) images of silica-coated iron oxide nanoparticles. Note that the final core/shell particles are rather monodisperse, even though most silica shells have trapped more than one magnetic core (see inset of Fig. 1) because of aggregation of the iron oxide nanoparticles prior to or during the coating process. The thickness of the silica shell can be tuned from a few to several hundreds of nanometers by simply varying the initial amount of TEOS. The silica-coated iron oxide particles used in this case for the production of luminescent magnetic particles had a core diameter of about 30 nm and a silica-shell thickness of 70 nm on average, yielding an average total diameter of 170 ± 10 nm.

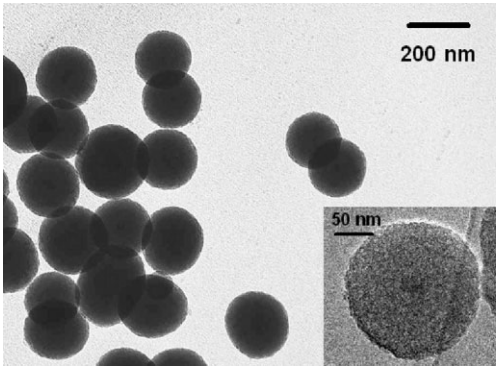

Figure 1. TEM images of silica-coated magnetite/maghemite nanoparticles. The higher-magnification image in the inset reveals that the cores are mainly made of small aggregates of the magnetic nanoparticles.

The magnetic properties of the silica-coated iron oxide spheres were recorded using a superconducting quantum interference device (SQUID) magnetometer with fields up to 5 T. Hysteresis loops of the samples were registered at temperatures of 5 and 300 K (Fig. 2A). At 5 K, the core/shell particles exhibited ferromagnetic characteristics, including coercivity ($H_c = 175$ Oe; 1 Oe $= 1000/4\pi$ A m^{-1}) and remanence. These magnetic silica spheres are superparamagnetic at room temperature, reaching a saturation moment of 1.34 emu per gram of material (silica and iron oxide). This low saturation magnetization value, far less than the saturation magnetization of the magnetite/maghemite nanoparticles used for the preparation of these core/shell spheres (54 emu g^{-1}), can be explained by taking into account the diamagnetic contribution of the thick silica shell surrounding the magnetic cores (the magnetic cores amount to only 2 wt.-% of a magnetic silica sphere). The temperature dependence of the zero-field-cooled/field-cooled (ZFC/FC) magnetization is shown in Figure 2B. Both curves coincide at high temperature and begin to separate as the temperature decreases, showing a maximum (in the case of the ZFC curve) at 120 K. Such behavior is characteristic of superparamagnetism[25] and is due to the progressive deblocking of particles as the temperature increases. It is generally assumed that the temperature at the maximum depends on the average particle size, while the temperature at which the FC and ZFC curves start to separate corresponds to the blocking temperature of the largest particles. The difference between both temperatures ($T_{max} = 120$ K and $T_B = 150$ K, respectively) represents,

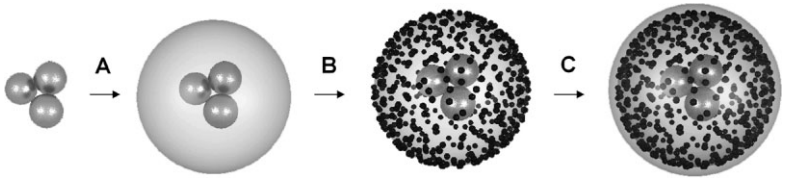

Scheme 1. Preparation of the magnetic and luminescent nanocomposite particles.

ADVANCED FUNCTIONAL MATERIALS

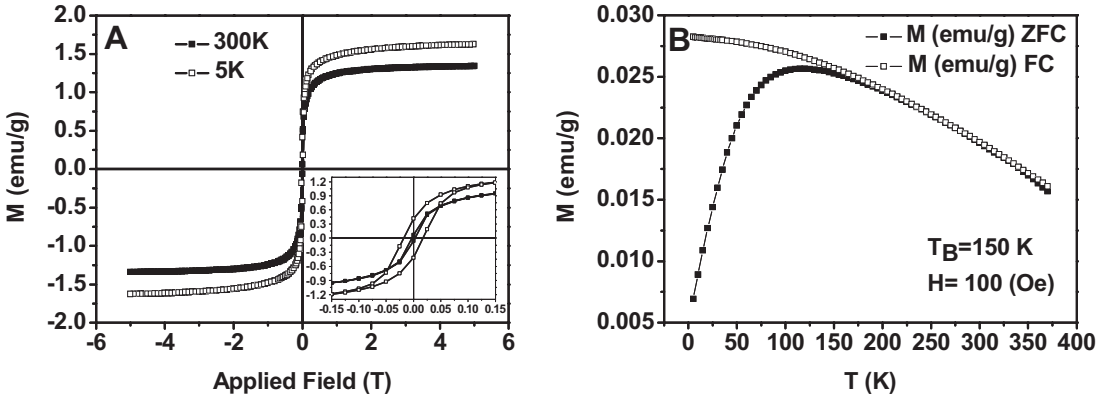

Figure 2. Magnetic measurements of core/shell magnetic silica spheres showing A) magnetization–applied magnetic field (*M*–*H*) and B) zero-field-cooled (ZFC) and field-cooled (FC) magnetization curves. The inset in (A) is a magnified view of the magnetization curves at low applied fields. 1 Oe = 1000/4π A m^{-1}; T_B: blocking temperature.

therefore, a qualitative measure of the magnetic-core size distribution in the silica spheres. These magnetic properties will allow the nanoparticles to be used in biomedical applications since they undergo strong magnetization, allowing for efficient magnetic separation under an applied external magnetic field, as shown below.

The formation of CdTe nanocrystals requires reflux of QD precursors[9b] at 100 °C, and the reflux time determines the final particle size. Here we have used two samples which were refluxed for 1.5 h (sample 1, 3 nm average diameter) and 20 h (sample 2, 5 nm average diameter). The duration of the heat treatment necessary to reach a certain particle size depends on the nature of the stabilizer, which, in this case, was thioglycolic acid. Figure 3 shows typical absorption and room-temperature photoluminescence (PL) spectra of both samples (samples 1,2) of CdTe nanocrystals in aqueous solution, measured from as-prepared CdTe colloidal solutions that were taken from the refluxing reaction at the two selected time intervals (1.5 and 20 h). The absorption spectra (Fig. 3A) show a peak corresponding to the first excitonic transition. Both samples also show a well-resolved PL band (maxima at 567 and 623 nm for samples 1,2, respectively) indicating a sufficiently narrow size distribution of the CdTe QDs.

CdTe QDs were deposited onto the surface of the silica-coated iron oxide particles by using a well-established method for the assembly of nanoparticles on colloidal spheres (Scheme 1B).[26] The method consists of depositing a precursor multilayer polyelectrolyte film, PDADMAC/PSS/PDADMAC (PDADMAC: poly(diallyldimethyl ammonium chloride); PSS: poly(sodium 4-styrenesulfonate), onto the magnetic silica spheres to generate a uniform surface charge and smooth coating, followed by depositing the CdTe QDs. Driven by electrostatic interactions, positively charged PDADMAC and negatively charged PSS were alternatively deposited onto the surface of the silica-coated iron oxide nanoparticles, forming a uniform polyelectrolyte layer. The CdTe nanocrystals of two different sizes were then assembled onto the surface of the spheres forming monolayers, again by means of electrostatic interactions between the negatively charged surfaces of the

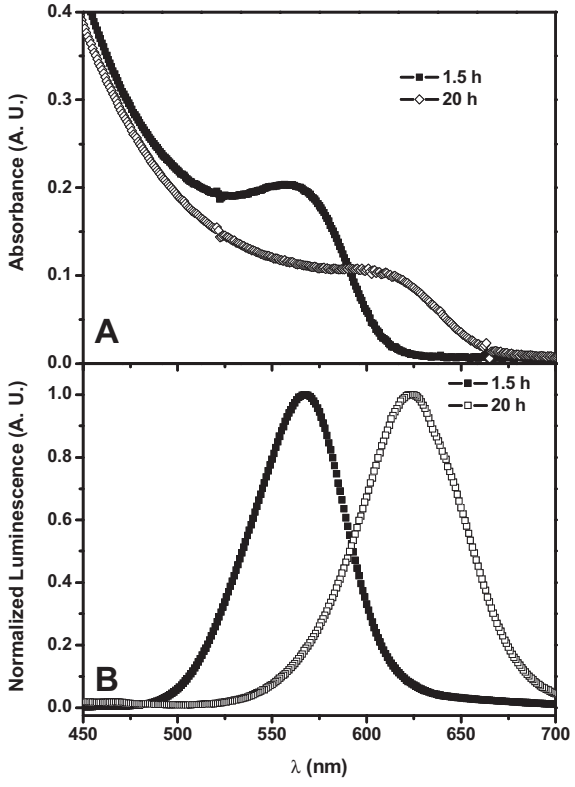

Figure 3. Absorption (A) and PL (B) spectra of CdTe QDs after refluxing the precursors for 1.5 (Sample 1) and 20 h (Sample 2). λ: wavelength.

CdTe nanocrystals and the positive charges on the outer layer of the PDADMAC polyelectrolyte. TEM images (Fig. 4) reveal a rougher surface of the silica-coated iron oxide nanoparticles as a result of the presence of the QDs.

The PL of the original QD dispersions was retained in the luminescent magnetic composites. The normalized PL emission spectra of the QDs (samples 1,2) and the luminescent magnetic

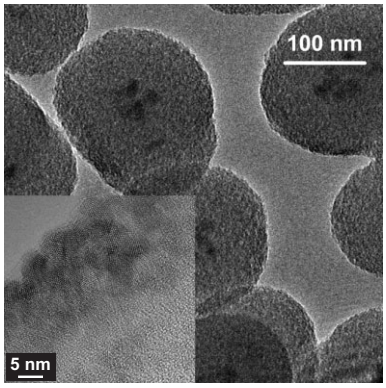

Figure 4. TEM image of QD-coated magnetic silica spheres. Inset: High-resolution TEM image of deposited CdTe QDs on the magnetic silica spheres.

composite particles are compared in Figure 5. The maxima of the emission spectra are blue-shifted (around 5 nm in both cases) compared to those of the free QDs in aqueous solution after assembling the CdTe QDs on the surfaces of the magnetic silica spheres. This behavior was already observed for CdSe QDs.[8d,27] Wang et al.[8d] reported blue-shifts both in absorption and luminescence spectra of CdSe and CdSe@CdS nanocrystals after treatment with light, which occurred as a result of a possible decrease in particle size during illumination. They explained the increase of quantum yield and the blue-shifts in the absorption and luminescence spectra by photoactivation processes that the QDs may have undergone, leading to annealing/restructuring of their surfaces and thereby removal of defects, since the photoactivation is accompanied by photocorrosion. On the other hand, thiol-capped CdTe QDs in solution show higher photostability in the presence of an excess of free thiol stabilizer.[9b] However, in this case, the thiol ligands may be converted to disulfides under irradiation and during the LbL process, producing unprotected CdTe QDs on the surfaces of the magnetic silica spheres, a fact that would explain the spectral shifts toward shorter wavelengths. On the other hand, we cannot provide reasonably accurate values for the quantum yield since the increase in light scattering once the QDs have been deposited onto the magnetic silica spheres complicates its quantification.

Luminescent silica nanoparticles have previously been synthesized by incorporating organic dyes into a silica matrix using a modified sol–gel procedure.[28] However, organic dyes[2b] are less bright, exhibit shorter photostability, and show broader emission peaks compared to semiconductor nanocrystals. Different approaches have also been reported for the deposition of QDs onto the surfaces of iron oxide nanoparticles, either by means of the LbL self-assembly technique[29] or using thiol chemistry.[30] In the first case, the system exhibited PL that was very sensitive to the distance between the Fe_3O_4 nanoparticles and the CdTe QDs; this interaction was suppressed when the maximum luminescence intensity was achieved, only after having deposited 21 layers of polyelectrolyte between the magnetic and luminescent nanoparticles. This fact may render this system very limited due to the highly time-consuming sequential polyelectrolyte-deposition cycles and purification steps.[31] In the second case, the authors found that running the coupling reaction between luminescent and magnetic nanoparticles in a mixture of chloroform/methanol/water resulted in partial aggregation of the composites. Herein, however, the silica shell grown between the magnetic material and the QDs prevents them from interacting with each other, thereby obtaining luminescent magnetic particles with the strongest PL. Furthermore, the high stability of the nanocomposites avoids any type of aggregation.

To further improve the colloidal and chemical stability,[32] the composite magnetic luminescent spheres were further coated with an outer layer of silica (20 nm average thickness) (Scheme 1C). To elucidate how the silica coating affects the PL, PL spectra of the composite particles were measured before and after the deposition of the outer silica shell (Fig. 6). Again, a blue-shift of the emission spectra (10 nm) was observed. Previous reports showed different results concerning the effect of the silica coating on the luminescent properties of QDs. It has been demonstrated[22a] that silica-coated CdS QDs undergo slower photodegradation compared to the same

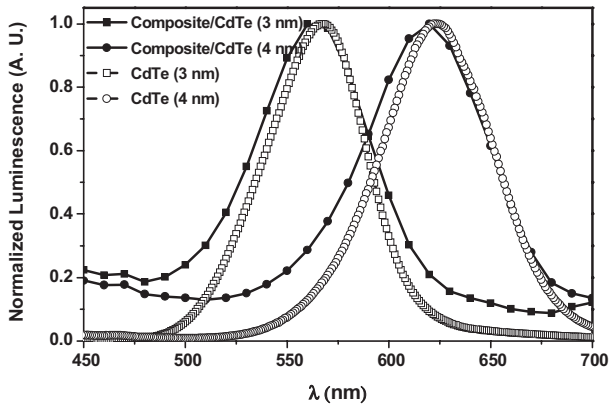

Figure 5. PL spectra of CdTe QDs (samples 1 and 2) before (open symbols) and after (solid symbols) deposition on the magnetic silica spheres.

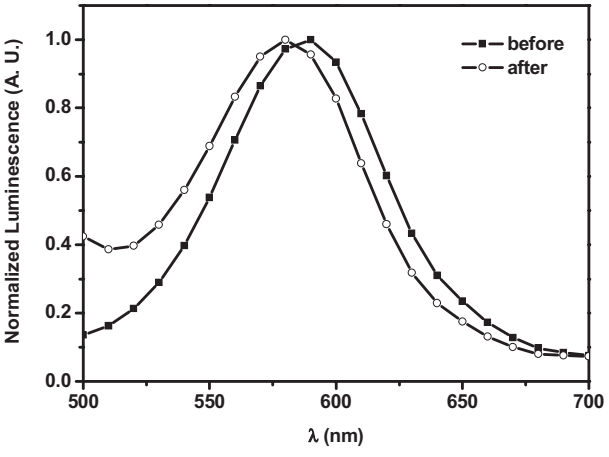

Figure 6. PL spectra of magnetic/luminescent composite particles before and after coating with an outer silica shell.

ADVANCED FUNCTIONAL MATERIALS

uncoated sample. However, Wang et al.[8d] observed a larger blue-shift (36 nm) in CdSe@CdS@SiO_2 nanoparticles compared with uncoated particles. Since we are comparing three different types of QDs (CdS, CdSe@CdS, CdTe) and different capping agents, different behavior is to be expected. In the case of CdTe nanocrystals, they may undergo further corrosion during silica deposition since thiol ligands must be completely removed from their surfaces, leaving the QDs entirely unprotected and resulting in this blue-shift in the maximum of the emission spectra.

Even if the outer silica shell cannot prevent corrosion of the CdTe QDs, it does improve the chemical and colloidal stability of the composite luminescent magnetic particles and offers an ideal anchorage substrate for the covalent binding of specific ligands.

Because of the magnetic iron oxide core, the composite particles can be directed to specific locations when manipulated by an external magnetic field, which, in this case, can be easily monitored through the intense luminescence of the composite particles. Figure 7 shows a series of photographs of an aqueous dispersion of luminescent magnetic spheres under UV illumination and illustrates the mentioned manipulation ability. While in the absence of a magnetic field the luminescence is observed from the whole dispersion (Fig. 7, left), when a handheld magnet is placed below the glass vial, the particles accumulate near it over a period of a few hours (Fig. 7, center). Once the particles have been concentrated close to the magnet, they can be easily dragged by moving the magnet to a different position (Fig. 7, right).

3. Conclusions

In summary, we have reported the synthesis of water-based luminescent magnetic colloidal particles. Such multifunctional nanocomposites, addressable by a magnetic field and detectable by their PL, were prepared by the encapsulation of both magnetic iron oxide nanoparticles and luminescent semiconductor nanocrystals within composite silica spheres. These QD-patterned magnetic silica spheres are expected to serve as luminescent markers while attached to bioligands and are capable of being driven by a magnetic field to a specific target.

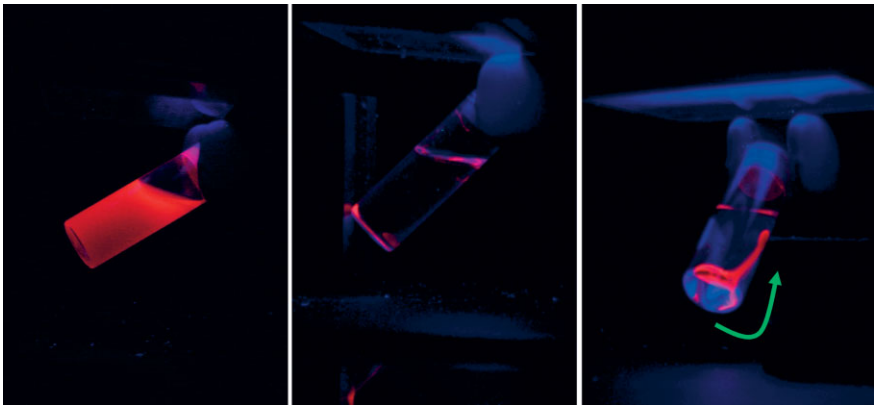

Figure 7. Photographs of luminescent magnetic silica spheres driven by an external magnetic field. No magnetic field applied (left); a handheld magnet placed below the sample for 2 h (center); movement of the magnet dragging the concentrated particle phase (right).

4. Experimental

Fe_3O_4 Nanoparticles: Aqueous dispersions of magnetite nanoparticles were prepared according to Massart's method [33], based on the co-precipitation of ferrous and ferric ion solutions (1:2 molar ratio). 20 mL of aqueous 1 M $FeCl_3$ (97 %, Aldrich) and 5 mL of 2 M $FeSO_4 \cdot 7H_2O$ (99 %, Riedel-de-Haen) in 2 M HCl were added to 250 mL of 0.7 M NH_4OH (28–30 %, Aldrich) under rapid mechanical stirring. Stirring was allowed to continue for 30 min, and then the black solid product was allowed to precipitate. The sediment was redispersed in 50 mL distilled water, and subsequently three aliquots of 10 mL tetramethylammonium hydroxide solution (10 % in water, Aldrich) (1 M) were added, again with rapid stirring. Finally, water was added to the dispersion up to a total volume of 250 mL. The magnetite nanoparticles (which were partially oxidized to maghemite) were further washed as follows: 4 mL of magnetic-nanoparticles solution was diluted with 36 mL distilled water containing 50 μL HCl (0.01 M), centrifuged, and redispersed in pure water.

Silica-Coated Magnetite/Maghemite Particles (Fe_3O_4/γ-Fe_2O_3@SiO_2): To a mixture of 4.85 mL NH_4OH (28 %), 28.8 mL H_2O, 27.5 mL EtOH, and 6.22 mL of the previously washed magnetic nanoparticles in aqueous solution, an ethanolic solution of TEOS (98 %, Aldrich) (2 mL of TEOS in 30 mL of EtOH) was added while mechanically stirring. After mixing, the final volume was 100 mL and the concentration of TEOS, NH_4OH, and H_2O were, respectively, 0.25, 0.35, and 21.4 M. The hydrolysis and condensation of TEOS onto the magnetic nanoparticles was completed in 4 h. The formed particles were centrifuged to eliminate excess reactants and redispersed in 50 mL of pure water. These core/shell magnetic silica spheres had an average diameter of 170 ± 10 nm.

CdTe QDs: Thioglycolic acid-stabilized CdTe QDs were synthesized as described elsewhere [9b]. The duration of the heat treatment necessary to reach a certain particle size was 1.5 h for sample 1 and 20 h for sample 2, which exhibited luminescence maxima at 567 and 623 nm, respectively. The average diameters of the CdTe QDs were approximately 3 and 5 nm for samples 1,2, respectively, as determined by TEM.

Semiconductor-Coated Magnetic Silica Spheres: The magnetic silica spheres were first covered by a supporting polyelectrolyte (PE) film by the alternate adsorption of PDADMAC (poly(diallyldimethyl ammonium chloride)) (weight-average molecular weight, M_w: 100 000–200 000, 20 % in water, Aldrich), PSS (poly(sodium 4-styrenesulfonate)) (M_w: 70 000, Aldrich) and PDADMAC, as described elsewhere [26], with a dominating influence of electrostatic interactions. These three layers of polyelectrolytes provided a smoother, more uniform, and positively charged surface on the magnetic silica spheres for deposition of the QDs. 0.5 mL of the PE-coated magnetic silica spheres (2.4 mg mL^{-1}) was dispersed in 0.5 mL of a 0.2 M NaCl solution, and then 1 mL of either sample 1 or sample 2 of CdTe QDs dispersions (as synthesized) was added. An adsorption time of 20 min was then allowed, and excess QDs were removed by three repeated centrifugation/wash cycles.

Silica-Coated Magnetic/Luminescent Particles: QD-patterned magnetic silica spheres were encapsulated with an outer shell of silica in a mixture of water/ethanol (1:4) containing 3-aminopropyl trimethoxysilane (Aldrich)

(APS, 15 μL) and TEOS (15 μL) as a result of the hydrolysis and condensation of the silanes on the surface of the composite spheres, as described elsewhere [34]. These conditions produced an outer silica shell with an average thickness of 20 nm.

Received: August 24, 2005
Final version: September 28, 2005
Published online: January 24, 2006

[1] a) H. Weller, *Angew. Chem. Int. Ed. Engl.* **1993**, *32*, 41. b) A. P. Alivisatos, *J. Phys. Chem.* **1996**, *100*, 13 226.

[2] a) M. Bruchez, Jr., M. Moronne, P. Gin, S. Weiss, A. P. Alivisatos, *Science* **1998**, *281*, 2013. b) W. C. W. Chan, S. Nie, *Science* **1998**, *281*, 2016. c) H. Mattoussi, J. M. Mauro, E. R. Goldman, G. P. Anderson, V. C. Sundar, F. V. Mikulec, M. G. Bawendi, *J. Am. Chem. Soc.* **2000**, *122*, 12 142. d) D. Gerion, F. Pinaud, S. C. Williams, W. J. Parak, D. Zanchet, S. Weiss, A. P. Alivisatos, *J. Phys. Chem. B* **2001**, *105*, 8861. e) N. N. Mamedova, N. A. Kotov, A. L. Rogach, J. Studer, *Nano Lett.* **2001**, *1*, 281. f) X. Michalet, F. F. Pinaud, L. A. Bentolila, J. M. Tsay, S. Doose, J. J. Li, G. Sundaresan, A. M. Wu, S. S. Gambhir, S. Weiss, *Science* **2005**, *307*, 538. g) S. T. Selvan, T. T. Tan, J. Y. Ying, *Adv. Mater.* **2005**, *17*, 1620.

[3] S. Pathak, S. K. Choi, N. Arnheim, M. E. Thompson, *J. Am. Chem. Soc.* **2001**, *123*, 4103.

[4] a) S. Kim, M. G. Bawendi, *J. Am. Chem. Soc.* **2003**, *125*, 14 652. b) W. Guo, J. J. Li, Y. A. Wang, X. Peng, *Chem. Mater.* **2003**, *15*, 3125. c) F. Pinaud, D. King, H.-P. Moore, S. Weiss, *J. Am. Chem. Soc.* **2004**, *126*, 6115.

[5] X. Gao, Y. Cui, R. M. Levenson, L. W. K. Chung, S. Nie, *Nat. Biotechnol.* **2004**, *22*, 969.

[6] T. Pellegrino, L. Manna, S. Kudera, T. Liedl, D. Koktysh, A. L. Rogach, S. Keller, J. Radler, G. Natile, W. J. Parak, *Nano Lett.* **2004**, *4*, 703.

[7] F. Osaki, T. Kanamori, S. Sando, T. Sera, Y. Aoyama, *J. Am. Chem. Soc.* **2004**, *126*, 6520.

[8] a) J. O. Winter, N. Gomez, S. Gatzert, C. E. Schmidt, B. A. Korgel, *Colloids Surf. A* **2005**, *254*, 147. b) A. Shavel, N. Gaponik, A. Eychmüller, *J. Phys. Chem. B* **2004**, *108*, 5905. c) Z. H. Zhang, W. S. Chin, J. J. Vittal, *J. Phys. Chem. B* **2004**, *108*, 18 569. d) Y. Wang, Z. Tang, M. A. Correa-Duarte, I. Pastoriza-Santos, M. Giersig, N. A. Kotov, L. M. Liz-Marzan, *J. Phys. Chem. B* **2004**, *108*, 15 461.

[9] a) A. L. Rogach, L. Katsikas, A. Kornowsik, D. Su, A. Eychmüller, H. Weller, *Ber. Bunsen-Ges.* **1996**, *100*, 1772. b) N. Gaponik, D. V. Talapin, A. L. Rogach, K. Hoppe, E. V. Shevchenko, A. Kornowski, A. Eychmüller, H. Weller, *J. Phys. Chem. B* **2002**, *106*, 7177.

[10] Y. R. Chemla, H. L. Crossman, Y. Poon, R. McDermott, R. Stevens, M. D. Alper, J. Clarke, *Proc. Natl. Acad. Sci. USA* **2000**, *97*, 14 268.

[11] a) C. Bergemann, D. Muller-Schulte, J. Oster, L. A. Brassard, A. S. Lubbe, *J. Magn. Magn. Mater.* **1999**, *194*, 45. b) K. Rudi, F. Larsen, K. S. Jakobsen, *Appl. Environ. Microbiol.* **1998**, *64*, 34.

[12] J. Ugelstad, A. Berge, T. Ellingsen, R. Schmid, T.-N. Nilsen, P. C. Mork, P. Stenstad, E. Hornes, O. Olsvik, *Prog. Polym. Sci.* **1992**, *17*, 87.

[13] D. R. Baselt, G. U. Lee, M. Natesan, S. W. Metzger, P. E. Sheehan, R. J. Colton, *Biosens. Bioelectron.* **1998**, *13*, 731.

[14] F. C. MacKintosh, C. F. Schmidt, *Curr. Opin. Colloid Interface Sci.* **1999**, *4*, 300.

[15] a) Q. A. Pankhurst, J. Connolly, S. K. Jones, J. Dobson, *J. Phys. D: Appl. Phys.* **2003**, *36*, R167. b) *Scientific and Clinical Applications of Magnetic Carriers* (Eds: U. Hafeli, W. Schutt, J. Teller, M. Zborowski), Plenum Press, New York **1997**. c) P. Tartaj, M. P. Morales, S. Veintemillas-Verdaguer, T. González-Carreño, C. J. Serna, *J. Phys. D: Appl. Phys.* **2003**, *36*, R182.

[16] T.-J. Yoon, J. S. Kim, B. G. Kim, K. N. Yu, M.-H. Cho, J.-K. Lee, *Angew. Chem. Int. Ed.* **2005**, *44*, 1068.

[17] a) P. Tartaj, C. J. Serna, *J. Am. Chem. Soc.* **2003**, *125*, 15 754. b) P. Tartaj, T. González-Carreño, C. J. Serna, *Adv. Mater.* **2001**, *13*, 1620.

[18] G. Ennas, A. Musinu, G. Piccaluga, D. Zadda, D. Gatteschi, C. Sangregorio, J. L. Stanger, G. Concas, G. Spano, *Chem. Mater.* **1998**, *10*, 495.

[19] a) L. M. Liz-Marzán, M. Giersig, P. Mulvaney, *Langmuir* **1996**, *12*, 4329. b) T. Ung, L. M. Liz-Marzán, P. Mulvaney, *Langmuir* **1998**, *14*, 3740.

[20] a) M. P. B. van Bruggen, *Langmuir* **1998**, *14*, 2245. b) J. Perez-Juste, M. A. Correa-Duarte, L. M. Liz-Marzán, *Appl. Surf. Sci.* **2004**, *226*, 137.

[21] a) E. A. Whitsitt, A. R. Barron, *Nano Lett.* **2003**, *3*, 775. b) T. Seeger, P. Redlich, N. Grobert, M. Terrones, D. R. M. Walton, H. W. Kroto, M. Rühle, *Chem. Phys. Lett.* **2001**, *339*, 41.

[22] a) M. A. Correa-Duarte, M. Giersig, L. M. Liz-Marzán, *Chem. Phys. Lett.* **1998**, *286*, 497. b) M. A. Correa-Duarte, Y. Kobayashi, R. A. Caruso, L. M. Liz-Marzán, *J. Nanosci. Nanotechnol.* **2001**, *1*, 95.

[23] W. Stöber, A. Fink, E. Bohn, *J. Colloid Interface Sci.* **1968**, *26*, 62.

[24] P. A. Philipse, M. P. B. van Bruggen, C. Pathmamanoharan, *Langmuir* **1994**, *10*, 92.

[25] a) A. H. Morrish, *The Physical Principles of Magnetism*, Wiley, New York **1965**. b) S. Morup, F. Bodker, P. V. Hendriksen, S. Linderoth, *Phys. Rev. B* **1995**, *52*, 287.

[26] a) F. Caruso, H. Lichtenfeld, M. Giersig, H. Möhwald, *J. Am. Chem. Soc.* **1998**, *120*, 8523. b) F. Caruso, R. A. Caruso, H. Möhwald, *Science* **1998**, *282*, 1111. c) G. Decher, *Science* **1997**, *277*, 1232. d) N. A. Kotov, I. Dekany, J. H. Fendler, *J. Phys. Chem.* **1995**, *99*, 13 065.

[27] M. Nirmal, B. O. Dabbousi, M. G. Bawendi, J. J. Macklin, J. K. Trautman, T. D. Harris, L. E. Brus, *Nature* **1996**, *383*, 802.

[28] a) A. van Blaaderen, A. Vrij, *Langmuir* **1992**, *8*, 2921. b) N. A. M. Verhaegh, A. van Blaaderen, *Langmuir* **1994**, *10*, 1427.

[29] X. Hong, J. Li, M. Wang, J. Xu, W. Guo, J. Li, Y. Bai, T. Li, *Chem. Mater.* **2004**, *16*, 4022.

[30] D. Wang, J. He, N. Rosenzweig, Z. Rosenzweig, *Nano Lett.* **2004**, *4*, 409.

[31] F. Caruso, *Adv. Mater.* **2001**, *13*, 11.

[32] D. K. Yi, S. T. Selvan, S. S. Lee, G. C. Papaefthymiou, D. Kundaliya, J. Y. Ying, *J. Am. Chem. Soc.* **2005**, *127*, 4990.

[33] R. Massart, *IEEE Trans. Magn.* **1981**, *MAG-17*, 1247.

[34] V. Salgueiriño-Maceira, M. Spasova, M. Farle, *Adv. Funct. Mater.* **2005**, *15*, 1036.